A Comparison Between Uplink and Downlink MC-DS-CDMA Sensitivity to Static Timing and Clock Frequency Offsets

Heidi Steendam, Herwig Bruneel, and Marc Moeneclaey

***Abstract*—We study the effect of fixed timing offsets and clock frequency offsets on the performance of multicarrier direct-sequence CDMA (MC-DS-CDMA) for both uplink and downlink communication, assuming orthogonal spreading sequences and a slowly varying multipath channel. We point out that a constant timing offset does not give rise to performance degradation for neither uplink nor downlink MC-DS-CDMA. We derive simple but accurate approximate expressions that allow us to easily quantify the effect of clock frequency offset and the influence of the different system parameters on the receiver performance in practical situations. Further, we show that for both uplink and downlink MC-DS-CDMA, the performance in the presence of a clock frequency offset rapidly degrades with an increasing number of carriers. It turns out that this degradation is larger in the uplink than in the downlink because the former suffers from a higher level of multiuser interference. For a given maximum relative clock frequency offset, enlarging the spreading factor in a fully loaded system does not affect the downlink degradation but strongly increases the uplink degradation.**

***Index Terms*—Clock frequency offset, multicarrier direct-sequence CDMA, synchronization.**

I. Introduction

BECAUSE of the enormous growth of wireless services (cellular telephones, wireless local area networks, etc.) during the last decade, the need for a modulation technique that can reliably transmit high data rates at a high bandwidth efficiency arises. As multicarrier (MC) systems have good bandwidth efficiency and can offer immunity to channel dispersion, these techniques are excellent candidates for high data rate transmission over multipath channels [1]–[5]. In MC systems like orthogonal frequency-division multiplexing (OFDM), multicarrier code-division multiple access (MC-CDMA), and multicarrier direct-sequence code-division multiple access (MC-DS-CDMA), the available bandwidth is partitioned in a large number of orthogonal subchannels or carriers [1]. The (de)modulation of the (spread) data on the carriers can be accomplished by means of fast Fourier transforms (FFTs). Further, a guard interval (cyclic prefix) is used to combat the frequency selectivity of the channel.

In the OFDM technique, the data sequence to be transmitted is split into a large number of lower rate data streams, each of which modulate a different carrier of the MC system [1]–[5]. The OFDM technique is not a multiple access technique, as all carriers are modulated with data from the same user. To support multiple users, the OFDM technique must be combined with a multiple access technique. In this context, the MC modulation technique has been investigated in combination with the CDMA technique [4]–[18]. Two of these combinations are MC-CDMA and MC-DS-CDMA. In MC-CDMA [4]–[11], the original data stream is first multiplied with the spreading sequence, and then, the different chips belonging to the same data symbol are modulated on different carriers: the spreading is done in the frequency domain. In MC-DS-CDMA [6], [10]–[18], on the other hand, the serial-to-parallel converted data stream is multiplied with the spreading sequence, and then, the chips belonging to the same symbol modulate the same carrier: The spreading is done in the time-domain. Both MC-CDMA and MC-DS-CDMA have been proposed for mobile radio communications [4]–[18]. In this paper, we will focus on the MC-DS-CDMA system.

The use of a large number of carriers makes multicarrier systems very sensitive to carrier and clock frequency offsets. In [19]–[24], the effect of *carrier* frequency offsets on various multicarrier systems has been investigated. The sensitivity to *clock* frequency offsets has been reported for OFDM and MC-CDMA in [19], [25]–[27] and for *downlink* MC-DS-CDMA in [28]. The present paper extends results from [28] by examining the effect of static clock phase offsets and clock frequency offsets on both *uplink* and *downlink* MC-DS-CDMA. In addition, we derive simple but accurate expressions for the degradation caused by the considered timing errors that allow us to easily quantify the influence of the various system parameters on this degradation.

The paper is organized as follows. In Section II, we describe the uplink and downlink MC-DS-CDMA systems operating on a multipath fading channel. In Section III, we investigate the effect of constant timing offsets on uplink and downlink transmission. We derive, in Section IV, exact expressions for the performance degradation caused by clock frequency offsets in uplink and downlink MC-DS-CDMA and present simple approximations thereof. The conclusions are drawn in Section V. One of the main conclusions is that MC-DS-CDMA is much more sensitive to clock frequency offsets in the uplink than in the downlink, especially when the spreading factor is large.

Manuscript received July 5, 2004; revised November 19, 2004. This work was supported by the Interuniversity Attraction Poles Program P5/11 Belgian Science Policy and was presented in part at the IEEE International Symposium on Spread Spectrum Techniques and Applications, Prague, Czech Republic, September 2002. The associate editor coordinating the review of this paper and approving it for publication was Dr. Markus Rupp.

The authors are with the Telecommunications and Information Processing (TELIN) Department, Ghent University, B-9000 Gent, Belgium (e-mail: Heidi.Steendam@telin.ugent.be; hs@telin.ugent.be; hb@telin.ugent.be; mm@telin.ugent.be).

Digital Object Identifier 10.1109/TSP.2005.855402

1053-587X/$20.00 © 2005 IEEE

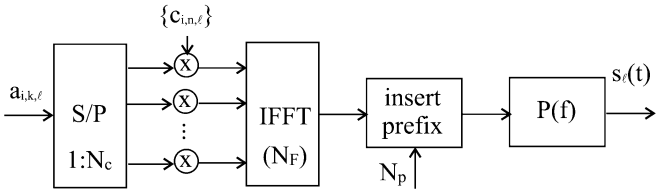

Fig. 1. MC-DS-CDMA transmitter structure for a single user.

II. System Description

A. Uplink MC-DS-CDMA

The conceptual block diagram of the transmitter of an MC-DS-CDMA system for a single user is shown in Fig. 1. In MC-DS-CDMA, the complex data symbols to be transmitted at rate R_s are first split into N_c symbol sequences at rate R_s/N_c. Each of these lower rate symbol sequences modulates a different carrier of the orthogonal multicarrier system. We denote by $a_{i,k,\ell}$ the data symbol transmitted by user ℓ on carrier k during the ith symbol interval; k belongs to a set I_c of N_c carrier indices. The data symbol $a_{i,k,\ell}$ is then multiplied with a higher rate spreading sequence $\{c_{i,n,\ell}\,|\,n=0,\ldots,N_s-1\}$ with spreading factor N_s, where $c_{i,n,\ell}$ denotes the nth chip of the sequence that spreads the data symbols from user ℓ during the ith symbol interval. Note that the spreading sequence does not depend on the carrier index k: All N_c data symbols from user ℓ that are transmitted during the same symbol interval of duration N_c/R_s are spread with the same spreading sequence. It is assumed that $|c_{i,n,\ell}|=1$. We denote by $\{b_{i,n,k,\ell}\,|\,n=0,\ldots,N_s-1\}$ the N_s components of the spread data symbol $a_{i,k,\ell}$, i.e.,

$$b_{i,n,k,\ell}=\frac{1}{\sqrt{N_s}}a_{i,k,\ell}c_{i,n,\ell},\quad n=0,\ldots,N_s-1;k\in I_c. \quad (1)$$

The components $b_{i,n,k,\ell}$ are serially transmitted on the kth carrier of an orthogonal multicarrier system, i.e., the spreading is done in the time-domain (see Fig. 2). (This is in contrast to MC-CDMA, where the spreading is done in the frequency domain.) Each component $b_{i,n,k,\ell}$ has a duration $(N_c/N_s)/R_s$. To modulate the spread data symbols on the orthogonal carriers, an N_F-point inverse fast Fourier transform (inverse FFT) is used. To avoid the fact that the multipath channel causes interference between the data symbols at the receiver, each FFT block at the inverse FFT output is cyclically extended with a prefix of N_p samples. This results in the sequence of samples $\{s_{i,n,m,\ell}\,|\,m=-N_p,\ldots,N_F-1\}$ given by

$$s_{i,n,m,\ell}=\frac{1}{\sqrt{N_F+N_p}}\sum_{k\in I_c}b_{i,n,k,\ell}e^{j2\pi\frac{km}{N_F}}. \quad (2)$$

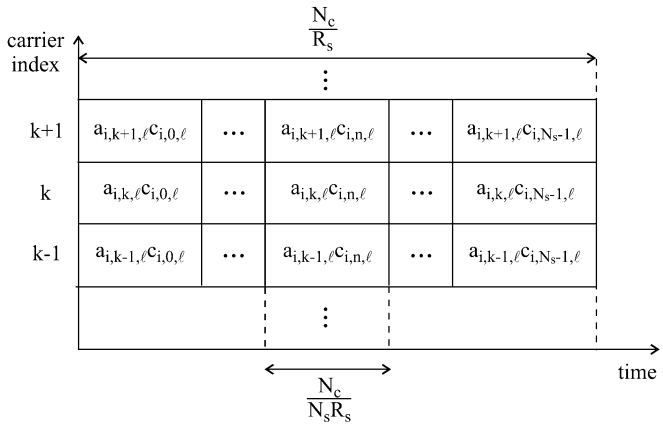

Fig. 2. Time-domain spreading in MC-DS-CDMA.

The sequence $\{s_{i,n,m,\ell}\,|\,m=-N_p,\ldots,N_F-1\}$ is fed to a square-root raised-cosine filter $P(f)$ with rolloff α and unit-energy impulse response $p(t)$, with $P(f)=\sqrt{G(f)}$, and $G(f)$ [which has one-sided bandwidth $(1+\alpha)/2T$] is given by (3) (see [29]), shown at the bottom of the page. The resulting continuous-time transmitted complex baseband signal $s_\ell(t)$ is given by

$$s_\ell(t)=\sum_{i=-\infty}^{+\infty}\sum_{m=-N_p}^{N_F-1}\sum_{n=0}^{N_s-1}s_{i,n,m,\ell}\cdot p(t-(m+(n+iN_s)(N_F+N_p))T-\tau_{i,n,m,\ell}) \quad (4)$$

where $1/T=(N_F+N_p)N_sR_s/N_c$ is the network reference clock frequency, and $\tau_{i,n,m,\ell}$ is a time-varying delay representing the transmit clock phase of user ℓ. Because of the normalization factors introduced in (1) and (2), the transmitted energy per symbol on the kth carrier from user ℓ is given by $E_{s,k,\ell}=E[|a_{i,k,\ell}|^2]$. In the following, it is assumed that carriers inside the roll-off area of the transmit filter are not modulated, i.e., they have zero amplitude. Hence, of the N_F available carriers, only N_c carriers are actually used $(N_c\le(1-\alpha)N_F)$. Assuming N_c to be odd, the set I_c of carriers actually used is given by $I_c=\{0,\ldots,(N_c-1)/2\}\cup\{N_F-(N_c-1)/2,\ldots,N_F-1\}$. The corresponding carrier spacing Δf and system bandwidth B are given by

$$\Delta f=\frac{1}{N_FT}=\frac{N_s}{N_c}R_s\frac{N_F+N_p}{N_f}\approx\frac{N_s}{N_c}R_s$$
$$B=N_c\Delta f=\frac{N_c}{N_FT}=N_sR_s\frac{N_F+N_p}{N_f}\approx N_sR_s. \quad (5)$$

The above approximations are valid for $N_p\ll N_F$.

In a multiuser scenario, each user transmits to the basestation a similar signal $s_\ell(t)$. To separate the different user signals

$$G(f)=\begin{cases}T, & |f|T\le\dfrac{(1-\alpha)}{2}\\ \dfrac{T}{2}\left(1-\sin\left(\dfrac{\pi}{\alpha}\left(|f|T-\dfrac{1}{2}\right)\right)\right), & \frac{(1-\alpha)}{2}\le|f|T\le\frac{(1+\alpha)}{2}\\ 0, & \text{otherwise.}\end{cases} \quad (3)$$

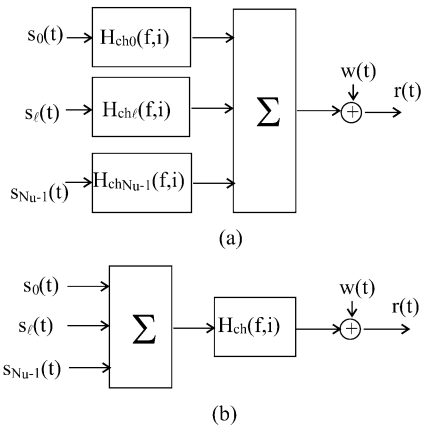

Fig. 3. Channel structure for (a) uplink and (b) downlink.

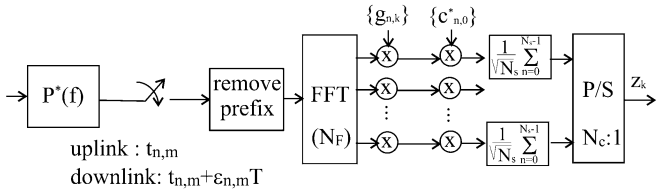

Fig. 4. MC-DS-CDMA receiver structure.

at the basestation receiver, each user is assigned a unique spreading sequence $\{c_{i,n,\ell}\}$, with ℓ denoting the user index. In this contribution, we consider orthogonal sequences, consisting of user-dependent Walsh–Hadamard (WH) sequences of length N_s, multiplied with a complex-valued random scrambling sequence that is common to all N_u active users. Hence, the maximum number of users that can be accommodated equals N_s, i.e., the number of WH sequences of length N_s. Note that the number of carriers N_c can be chosen independently of the spreading factor N_s, which in turn equals the maximum number of users. Without loss of generality, we focus on the detection of the data symbols transmitted by the reference user ($\ell = 0$).

The signal $s_\ell(t)$ transmitted by user ℓ reaches the basestation through a slowly varying multipath channel. We assume that the path gains are constant over the duration N_c/R_s of N_s FFT blocks; the corresponding channel transfer function experienced by the ith FFT block from user ℓ is denoted $H_{\mathrm{ch},\ell}(f,i)$ [see Fig. 3(a)]. We restrict our attention to wide-sense stationary uncorrelated scattering (WSSUS); hence, the second-order moment $E[|H_{\mathrm{ch},\ell}(f;i)|^2]$ is independent of both f and i. The basestation receives the sum of the resulting user signals and an additive white Gaussian noise (AWGN) process $w(t)$. The real and imaginary parts of $w(t)$ are uncorrelated, and each has a power spectral density of $N_0/2$. The resulting signal is applied to the receiver filter, which is matched to the transmit filter, and sampled at the instants $t_{i,n,m} = (m + (n + iN_s)(N_F + N_p))T$ (see Fig. 4). Only the N_F samples with $m = 0, \ldots, N_F - 1$ are kept for further processing.

In uplink communication, a timing misalignment of the FFT blocks transmitted by the different users is present. However, it is assumed that this misalignment is kept within a small fraction of an FFT block by exploiting timing correction information sent by the basestation to the different users. The transmitter of each user adapts its transmit clock phase $\tau_{i,n,m,\ell}$ by means of coarse synchronization (to be explained in more detail in Section IV) such that the samples used for further processing are not affected by interference between successive FFT blocks. This adaptation introduces a timing offset $\epsilon_{i,n,m,\ell}T$, as compared with the sampling instants $t_{i,n,m}$ of the basestation. The contribution of each user is affected by a different timing offset $\epsilon_{i,n,m,\ell}T$, as each user signal is generated with a different transmit clock and is transmitted over a different multipath channel. For each user, it is assumed that the transmitter timing is between the earliest and latest transmitter timing indicated in Fig. 5(a) so that the N_F samples kept for further processing at the basestation are free from interference from neighboring blocks. This implies that the length of the cyclic prefix must be sufficiently longer than the maximum duration T_{ch} of the impulse responses of the composite channels with transfer functions $H_\ell(f,i) = |P(f)|^2 H_{\mathrm{ch},\ell}(f,i)$ ($\ell = 0, \ldots, N_u - 1$). As the removal of the cyclic prefix at the receiver eliminates the interference between neighboring blocks, the data symbols $a_{i,k,\ell}$ transmitted during symbol interval i are not affected by intersymbol interference from other symbol intervals. Hence, we omit the symbol index i in the sequel. The samples $r_{n,m}$ at the output of the receiver filter are given by

$$r_{n,m} = \sum_{\ell=0}^{N_u-1} \sum_{m'=0}^{N_F-1} \sum_{n'=0}^{N_s-1} s_{n',m',\ell} \cdot h_{\mathrm{ch},\ell}(((m-m') + (n-n')(N_F+N_p))T - \epsilon_{n',m',\ell}T) + w_{n,m} \quad (6)$$

where $h_{\mathrm{ch},\ell}(t)$ is the impulse response of the composite channel with transfer function $H_\ell(f)$, and $w_{n,m}$ are the filtered noise samples at the instants $(m + n(N_F + N_p))T$.

The N_F selected samples $\{r_{n,m} \,|\, m = 0, \ldots, N_F - 1\}$ are applied to an N_F-point FFT followed by one-tap equalizers $g_{n,k}$ that scale and rotate the FFT outputs. We denote by $g_{n,k}$ the coefficient of the equalizer operating on the kth FFT output during the nth FFT block. Each equalizer output is multiplied with the

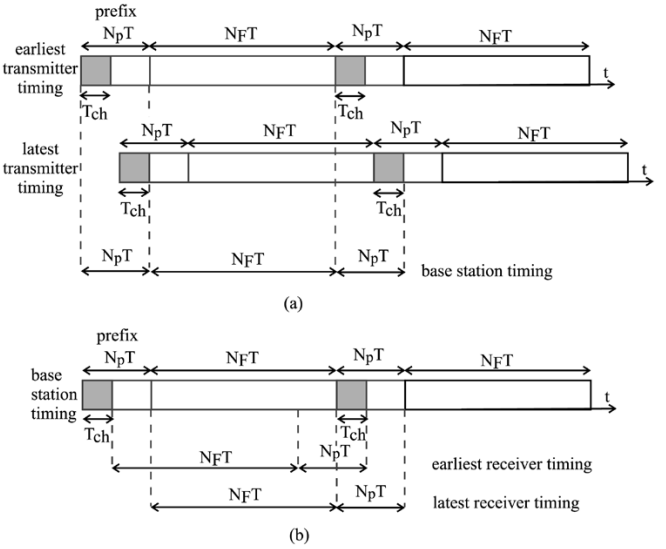

Fig. 5. Earliest and latest possible timing to avoid interference between FFT blocks. (a) Uplink. (b) Downlink.

corresponding chip of the reference user's spreading sequence, and the N_s consecutive values are summed to yield the samples z_k at the input of the decision device.

Denoting by $y_{n,k}$ the kth output of the FFT during the nth FFT block and taking (2) and (6) into account, we obtain

$$y_{n,k} = \frac{1}{\sqrt{N_F}} \sum_{m=0}^{N_F-1} r_{n,m} e^{-j2\pi \frac{km}{N_F}}, \quad k \in I_c$$
$$= \sqrt{\frac{N_F}{N_F+N_p}} \sum_{\ell=0}^{N_u-1} \sum_{k' \in I_c} b_{n,k',\ell} A_{n,k,k',\ell} + \tilde{w}_{n,k} \quad (7)$$

with

$$A_{n,k,k',\ell} = \frac{1}{N_F} \sum_{m=0}^{N_F-1} e^{-j2\pi \frac{m(k-k')}{N_F}} H_{k',\ell}(\epsilon_{n,m,\ell}) \quad (8)$$

$$H_{k,\ell}(\epsilon_{n,m,\ell}) = \frac{1}{T} \sum_{m'=-\infty}^{+\infty} H_\ell \left(\frac{k}{N_F T} + \frac{m'}{T} \right) \times e^{j2\pi \left(\frac{k}{N_F} + m' \right) \epsilon_{n,m,\ell}}. \quad (9)$$

The detection of the symbol $a_{k,0}$ is based on the decision variable z_k, which is given by

$$z_k = \frac{1}{\sqrt{N_s}} \sum_{n=0}^{N_s-1} y_{n,k} g_{n,k} c^*_{n,0}$$
$$= \sqrt{\frac{N_F}{N_F+N_p}} \sum_{\ell=0}^{N_u-1} \sum_{k' \in I_c} a_{k',\ell} I_{k,k',\ell} + W_k, \quad k \in I_c \quad (10)$$

where

$$I_{k,k',\ell} = \frac{1}{N_s} \sum_{n=0}^{N_s-1} c^*_{n,0} c_{n,\ell} g_{n,k} A_{n,k,k',\ell} \quad (11)$$

and W_k is the additive noise contribution, with

$$E[W_k W^*_{k'}] = N_0 \delta_{k-k'} \frac{1}{N_s} \sum_{n=0}^{N_s-1} |g_{n,k}|^2. \quad (12)$$

The quantity $I_{k,k',\ell}$ denotes the contribution from the data symbol $a_{k',\ell}$ to the sample z_k at the input of the decision device. The sample z_k from (10) contains a useful component with coefficient $I_{k,k,0}$. The quantities $I_{k,k',0}$ $(k' \neq k)$ correspond to intercarrier interference (ICI), i.e., the contribution from data symbols transmitted by the reference user on other carriers. For $\ell \neq 0$, the quantities $I_{k,k',\ell}$ correspond to multiuser interference (MUI), i.e., the contribution from data symbols transmitted by other users.

We consider the case of the maximum ratio combiner (MRC). In this case, the equalizer coefficients yield

$$g_{n,k} = A^*_{n,k,k,0} = \frac{1}{N_F} \sum_{m=0}^{N_F-1} H^*_{k,0}(\epsilon_{n,m,0}). \quad (13)$$

The MRC coefficients (13) maximize the ratio $|I_{k,k,0}|^2 / E[|W_k|^2]$, or, equivalently, the ratio of the useful signal power to noise power at the input of the decision device.

It is instructive to consider the case where all timing offsets are zero, i.e., $\epsilon_{n,m,\ell} = 0$ for $\ell = 0, \ldots, N_u - 1$. In this case, (8) and (9) reduce to

$$A_{n,k,k',\ell} = H_{k,\ell} \delta_{k-k'} \quad (14)$$

$$H_{k,\ell} = \frac{1}{T} \sum_{m'=-\infty}^{+\infty} H_\ell \left(\frac{k}{N_F T} + \frac{m'}{T} \right). \quad (15)$$

Hence, the contribution from user ℓ to the kth FFT output $y_{n,k}$ is proportional to $b_{n,k,\ell} H_{k,\ell}$, which means that ICI is absent. Further, as the factor $H_{k,\ell}$ does not depend on the chip index n, the orthogonality between the contributions from different users to the same FFT output is not affected, i.e., $I_{k,k',\ell} = 0$ for $\ell \neq 0$; hence, MUI is absent as well. At the input of the decision device, one obtains

$$z_k = \sqrt{\frac{N_F}{N_F+N_p}} a_{k,0} |H_{k,0}|^2 + W_k \quad \text{(no timing offsets)} \quad (16)$$

with $E[|W_k|^2] = N_0 |H_{k,0}|^2$. Hence, the signal-to-noise ratio (SNR) at the input of the decision device equals $(N_F/(N_F + N_p))|H_{k,0}|^2 (E_{s,k,0}/N_0)$. This indicates that in the absence of timing offsets, the multipath channel affects the SNR at the input of the decision device (through $|H_{k,0}|^2$) but does not give rise to interference.

B. Downlink MC-DS-CDMA

In downlink MC-DS-CDMA, the basestation synchronizes the N_u user signals ($\tau_{n,m,\ell} = 0$ for $\ell = 0, \ldots, N_u - 1$) and broadcasts the sum of the N_u user signals $s_\ell(t)$ from (4) to the different users. As shown in Fig. 3(b), this broadcast signal reaches the receiver of the reference user through a slowly fading multipath channel with transfer function $H_{\rm ch}(f, \tau)$. The output of the channel is disturbed by AWGN $w(t)$ with uncorrelated real and imaginary parts, each having a power spectral density of $N_0/2$. The resulting signal is applied to the receiver filter (see Fig. 4) in order to detect the data symbols transmitted to the reference user ($\ell = 0$). The sampling instants are denoted $t_{n,m} + \epsilon_{n,m} T$, where $t_{n,m} = (m + n(N_F + N_p))T$, and $\epsilon_{n,m} T$ is the deviation from $t_{n,m}$; $1/T$ is the network reference clock frequency. Only the samples with indices $m = 0, \ldots, N_F - 1$ are kept for further processing. The receiver adjusts its sampling clock phase by means of coarse synchronization (to be explained in more detail in Section IV), such that the sample corresponding to $m = 0$ is located between the earliest and latest receiver timing indicated in Fig. 5(b): The N_F samples to be processed are free from interference between successive blocks. This implies that the length of the cyclic prefix is sufficiently longer than the duration $T_{\rm ch}$ of the composite channel with transfer function $H(f, i) = |P(f)|^2 H_{\rm ch}(f, i)$. As for uplink transmission, the index i will be omitted in the sequel. The sample z_k at the input of the decision device is represented by (10), which contains a useful component (ICI), multiuser interference (MUI), and noise. The quantities $I_{k,k',\ell}$ are given by (11), with $\epsilon_{n,m,\ell}$ and $H_\ell(f)$ substituted by $\epsilon_{n,m}$ and $H(f)$, respectively. As in uplink communication, we consider the maximum ratio combiner, such that the equalizer coefficients $g_{n,k}$ are given by (13), with $\epsilon_{n,m,\ell}$ and $H_\ell(f)$ substituted by $\epsilon_{n,m}$ and $H(f)$, respectively.

III. Constant Timing Offset

A. Uplink MC-DS-CDMA

In this section, we investigate the effect of constant timing offsets $\epsilon_{n,m,\ell} = \epsilon_{0,\ell}$ on the performance of uplink MC-DS-CDMA. As $\epsilon_{n,m,\ell}$ is independent of the indices m and n, (8) and (9) reduce to

$$A_{n,k,k',\ell} = \delta_{k-k'} H_{k,\ell}(\epsilon_{0,\ell}) \tag{17}$$

$$H_{k,\ell}(\epsilon_{0,\ell}) = \frac{1}{T} \sum_{m'=-\infty}^{+\infty} H_\ell \left(\frac{k}{N_F T} + \frac{m'}{T} \right) e^{j2\pi \left(\frac{k}{N_F} + m' \right) \epsilon_{0,\ell}}. \tag{18}$$

The composite channels $H_\ell(f,\tau)$ are bandlimited: $H_\ell(f,\tau) = 0, |f| > (1+\alpha)/(2T), 0 \leq \alpha \leq 1$. Hence, for frequencies $k/(N_F T)$ outside the roll-off area, the sum (18) reduces to one contribution, i.e., $H_{k,\ell}(\epsilon_{0,\ell}) = H_{k,\ell} \exp(j2\pi\epsilon_{0,\ell} \bmod (k;N_F)/N_F)$, where $H_{k,\ell} = H_\ell(\bmod(k;N_F)/(N_F T), 0)/T$, and $\bmod(x;N_F)$ is the modulo-N_F reduction of x, yielding a result in the interval $[-N_F/2, N_F/2]$.

Hence, the only effect of a constant timing offset is a rotation over an angle $2\pi\epsilon_{0,\ell} \bmod (k;N_F)/N_F$ of the contribution of user ℓ at the kth FFT output. From (17), we observe that the constant timing offset does not introduce ICI ($A_{n,k,k',\ell} = 0$ for $k' \neq k$). Further, as the quantity $A_{n,k,k',\ell}$ is independent of the chip index n, the orthogonality between the contributions from the different users is not affected by the constant timing offsets, i.e., multiuser interference is absent as well ($I_{k,k',\ell} = 0$ for $\ell \neq 0$). The systematic phase rotation of the FFT outputs is compensated without loss of performance by rotating the kth FFT output over an (estimate of the) angle $-2\pi\epsilon_{0,0} \bmod (k;N_F)/N_F$, resulting in equalizer coefficients $g_{n,k}$ given by

$$g_{n,k} = e^{-j2\pi \frac{\bmod(k;N_F)}{N_F} \epsilon_{0,0}} H^*_{k,0}. \tag{19}$$

The resulting quantity z_k at the input of the decision device is again given by (16). Hence, the effect of a constant timing offset on uplink MC-DS-CDMA is compensated without reduction of the SNR by applying the appropriate counter-rotation to each FFT output.

B. Downlink MC-DS-CDMA

In the case of a constant timing offset in downlink MC-DS-CDMA, the timing offset is given by $\epsilon_{n,m} = \epsilon_0$. Equations (8) and (9) reduce to (17) and (18), with $\epsilon_{0,\ell}$ and $H_\ell(f)$ substituted by ϵ_0 and $H(f)$, respectively. Hence, a constant timing offset only introduces a carrier-dependent phase rotation of the FFT outputs but does not give rise to ICI or MUI. The systematic phase rotation of the FFT outputs in the downlink is compensated without reducing the SNR by applying the appropriate counter-rotation to each FFT output.

IV. Clock Frequency Offset

A. Uplink MC-DS-CDMA

Assuming that the transmitter of each user has a free-running clock with a relative clock frequency offset $\Delta T_\ell/T$, as compared with the frequency $1/T$ of the basestation clock, the timing deviation increases linearly with time: $\epsilon_{n,m,\ell} = \epsilon_{0,\ell} + (m + n(N_F + N_p))\Delta T_\ell/T$. Hence, an increasing misalignment in time between the transmitted and the received samples is introduced. To compensate for this increasing misalignment, a coarse synchronization is performed. In uplink MC-DS-CDMA, this coarse synchronization is done at the transmitter of each user, based on timing information received from the basestation. At the transmitter of each user, the number of samples in the prefix is increased (when $\Delta T_\ell < 0$) or reduced (when $\Delta T_\ell > 0$) such that the N_F successive samples selected by the basestation for further processing are not affected by interference from neighboring blocks. After coarse synchronization, the resulting timing deviation can be written as $\epsilon_{n,m,\ell} = \epsilon_{n,\ell} + m\Delta T_\ell/T$, where $\epsilon_{n,\ell}$ denotes the timing deviation of the first of the N_F samples of the considered block that are processed by the basestation. The coarse synchronization restricts $\epsilon_{n,\ell}$ to an interval $[x_{\min}, x_{\max}]$: $\epsilon_{n,\ell} = M(\epsilon_{0,\ell} + n(N_F + N_p)\Delta T_\ell/T)$, where $M(x)$ is the modulo reduction of x, yielding a result in the interval $[x_{\min}, x_{\max}]$, as shown in Fig. 6. In order to avoid interference between successive FFT blocks, we need $(x_{\max} - x_{\min})T \leq N_p T - T_{\text{ch}}$.

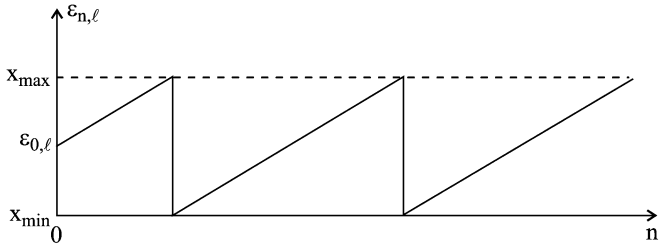

Fig. 6. Coarse synchronization $\Delta T > 0$.

For carriers outside the roll-off area, (11) reduces to

$$I_{k,k',\ell} = H^*_{k,0} H_{k',\ell} C^*_{k,k,0} C_{k,k',\ell} R_\ell(k,k') \tag{20}$$

where

$$C_{k,k',\ell} = D_{N_F} \left(\frac{k'-k}{N_F} + \frac{\bmod(k';N_F)}{N_F} \frac{\Delta T_\ell}{T} \right) \tag{21}$$

$$D_M(x) = \frac{1}{M} \sum_{m=0}^{M-1} e^{j2\pi mx} = e^{j\pi(M-1)x} \frac{\sin(\pi M x)}{M \sin(\pi x)} \tag{22}$$

$$R_\ell(k,k') = \frac{1}{N_s} \sum_{n=0}^{N_s-1} \tilde{c}_{n,k',\ell} \tilde{c}^*_{n,k,0} \tag{23}$$

$$\tilde{c}_{n,k,\ell} = c_{n,\ell} e^{j2\pi \frac{\bmod(k;N_F)}{N_F} \epsilon_{n,\ell}}. \tag{24}$$

In (20), $H_{k,\ell}$ is given by (15). The quantity $R_\ell(k,k')$ from (23) is the correlation between the sequences $\{\tilde{c}_{n,k',\ell}\}$ and $\{\tilde{c}_{n,k,0}\}$. In the sequence $\{\tilde{c}_{n,k,\ell}\}$, the chips $c_{n,\ell}$ are rotated over an angle $2\pi\epsilon_{n,\ell} \bmod (k;N_F)/N_F$, which depends on the chip index n, the carrier index k, and the timing deviation $\epsilon_{n,\ell}$ corresponding to the nth FFT block. Note that $R_0(k,k) = 1$. For $\ell \neq 0$, the chips $c_{n,\ell}$ of user ℓ and the chips $c_{n,0}$ of the reference user are rotated over different angles so that the orthogonality between the different user signals is destroyed: $R_\ell(k,k') \neq 0$ for $\ell \neq 0$. In the absence of clock frequency offsets, we have $C_{k,k',\ell} = \delta_{k,k'}$ and $|R_\ell(k,k')| = \delta_\ell$, whereas in the presence of clock frequency offsets, all $C_{k,k',\ell}$ and $R_\ell(k,k')$ are in general

nonzero. Hence, the clock frequency offsets give rise to both MUI and ICI.

Let us consider the signal to interference plus noise ratio (SINR) at the input of the decision device related to the carrier with index k. This yields

$$\mathrm{SINR}_k = \frac{\frac{N_F}{N_F+N_p}P_{U,k}}{N_0 + \frac{N_F}{N_F+N_p}(P_{\mathrm{ICI},k} + P_{\mathrm{MUI},k})} \tag{25}$$

where $P_{U,k}, P_{\mathrm{ICI},k}$, and $P_{\mathrm{MUI},k}$ are contributions from the useful signal, the ICI, and the MUI, respectively:

$$\begin{aligned} P_{U,k} &= E_{s,k,0}|H_{k,0}|^2|C_{k,k,0}|^2 \\ P_{\mathrm{ICI},k} &= \sum_{k'\in I_c, k'\neq k} E_{s,k',0}|H_{k',0}|^2|C_{k,k',0}|^2 E[|R_0(k,k')|^2] \\ P_{\mathrm{MUI},k} &= \sum_{\ell=1}^{N_u-1}\sum_{k'\in I_c} E_{s,k',\ell}|H_{k',\ell}|^2|C_{k,k',\ell}|^2 \\ &\quad \times E[|R_\ell(k,k')|^2]. \end{aligned} \tag{26}$$

The quantity SINR_k from (25) still depends on the particular realization of the transfer functions $H_{k,\ell}$ ($k \in I_c, \ell = 0,\ldots,N_u-1$) and of the spreading sequences during the considered sequence of N_s FFT blocks. Hence, a more convenient performance indicator is $\overline{\mathrm{SINR}}_k$, which is obtained from (25) by replacing $P_{U,k}, P_{\mathrm{ICI},k}$ and $P_{\mathrm{MUI},k}$ by their averages $\bar{P}_{U,k}, \bar{P}_{\mathrm{ICI},k}$ and $\bar{P}_{\mathrm{MUI},k}$ over the fading statistics and over all possible assignments of spreading sequences to the users. This averaging involves replacing in (26) $|H_{k,\ell}|^2$ and $|R_\ell(k,k')|^2$ by $E[|H_{k,\ell}|^2]$ and $E[|R_\ell(k,k')|^2]$, respectively.

We assume the application of power control so that in the absence of clock frequency offsets, all users achieve the same performance: The transmitted symbol energies $E_{s,k,\ell}$ are selected to compensate for the propagation loss differences between each user's transmitter and the receiver at the basestation, such that the average received symbol energies take the same value E_s for all users and all carriers: $E_{s,k,\ell}E[|H_{k,\ell}|^2] = E_s$. Because of the WSSUS assumption, $E[|H_{k,\ell}|^2]$ does not depend on the carrier index k; hence, the transmitted symbol energy $E_{s,k,\ell}$ depends on the user index ℓ but not on the carrier index k. In the absence of clock frequency offsets, $\overline{\mathrm{SINR}}_k = (N_F/(N_F+N_p))(E_s/N_0)$.

In the presence of clock frequency offsets, $\overline{\mathrm{SINR}}_k$ is less than $(N_F/(N_F+N_p))(E_s/N_0)$ because of the reduction of the useful component and the introduction of ICI and MUI. We define the degradation (in decibels) caused by the clock frequency offsets as $\mathrm{Deg}_k = 10\log((N_F/(N_F+N_p))(E_s/N_0)/\overline{\mathrm{SINR}}_k)$. Note that this degradation is a function of the carrier index k. This degradation corresponds to the increase of E_s/N_0 (or E_b/N_0) required to maintain the BER on the kth carrier in the presence of clock frequency offsets essentially the same as the BER in the absence of clock frequency offsets. In a well-designed system, this degradation should be in the order of 0.1 dB or less.

A necessary condition to keep the degradation small is that the useful component on each carrier of each user is only slightly affected by the clock frequency offsets, i.e., $|C_{k,k,\ell}|^2 \approx 1$ for all N_c carriers and all N_u users. Hence, assuming that $\Delta T_\ell/T$ is restricted to the interval $[-(\Delta T/T)_{\max}, (\Delta T/T)_{\max}]$ for $\ell = 0,\ldots,N_u-1$ and taking into account that the main lobe width (measured from $x=0$ to the first zero-crossing) of $D_M(x)$ from (22) equals $1/M$ (see Fig. 7), we require that $N_F(\Delta T/T)_{\max} \ll 1$ in order to guarantee that $|C_{k,k,\ell}|^2 \approx 1$. Further, as $D_M(m/M)$ is zero for integer m that are not a multiple of M, the condition $N_F(\Delta T/T)_{\max} \ll 1$ yields $|C_{k,k',\ell}|^2 \ll 1$ for $k' \neq k$ and $\ell = 0,\ldots,N_u-1$.

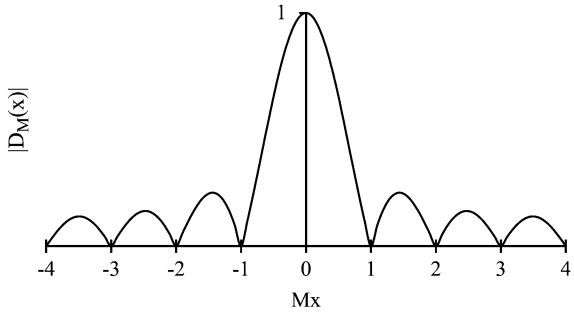

Fig. 7. Shape of $|D_M(x)|, M = 8$.

Now, we concentrate on $E[|R_\ell(k,k')|^2]$, which depends on the timing offsets $\epsilon_{n,\ell}$ at the beginning of the FFT blocks. For small clock frequency offsets, the dependence of $\epsilon_{n,\ell}$ on the index n is very weak; therefore, we expect $E[|R_\ell(k,k')|^2]$ to be close to its value corresponding to zero clock frequency offset: $E[|R_0(k,k')|^2] \approx 1$ and $E[|R_\ell(k,k')|^2] \ll 1$ for $\ell = 1,\ldots,N_u-1$. Let us assume that the clock frequency offsets are so small that $\epsilon_{0,\ell} + n(N_F+N_p)\Delta T_\ell/T$ is within the interval $[x_{\min}, x_{\max}]$ for all $n = 0,\ldots,N_s-1$ and all $\ell = 0,\ldots,N_u-1$. In this case, the timing offsets exhibit no jumps at the boundaries of the FFT blocks; therefore, $\epsilon_{n,\ell} = \epsilon_{0,\ell} + n(N_F+N_p)\Delta T_\ell/T$. This yields

$$E[|R_\ell(k,k')|^2] = \begin{cases} U_{k,k',0}, & \ell = 0 \\ \dfrac{1}{N_s-1}(1-U_{k,k',\ell}), & \ell \neq 0 \end{cases} \tag{27}$$

where

$$U_{k,k',\ell} = |D_{N_s}((N_F+N_p)q(k,k',\ell))|^2 \tag{28}$$

with

$$q(k,k',\ell) = \frac{\mathrm{mod}(k;N_F)\frac{\Delta T_0}{T} - \mathrm{mod}(k';N_F)\frac{\Delta T_\ell}{T}}{N_F}. \tag{29}$$

In the following, we investigate the contributions to $\bar{P}_{\mathrm{ICI},k}$ and $\bar{P}_{\mathrm{MUI},k}$, assuming small clock frequency offsets. In order to represent $|C_{k,k',\ell}|^2$ and $E[|R_\ell(k,k')|^2]$ accurately by a truncated Taylor series (keeping up to quadratic terms) around $\Delta T_0/T = \Delta T_\ell/T = 0$, we need $N_F(\Delta T/T)_{\max} \ll 1$ [see (21)] and $N_s(N_F+N_p)(\Delta T/T)_{\max} \ll 1$ [see (28)], respectively.

The contribution from carrier k' to $\bar{P}_{\mathrm{ICI},k}$ equals $\bar{P}_{\mathrm{ICI},k}(k') = E_s E[|R_0(k,k')|^2]|C_{k,k',0}|^2$. For $N_s(N_F+N_p)(\Delta T/T)_{\max} \ll 1$, one obtains from (21) and (27)

$$\bar{P}_{\mathrm{ICI},k}(k') \approx E_s A(k,k')\left(\frac{\Delta T_0}{T}\right)^2 \tag{30}$$

with

$$A(k,k') = \left(\frac{\pi \bmod (k';N_F)}{N_F \sin \frac{\pi(k-k')}{N_F}} \right)^2. \tag{31}$$

This indicates that the contribution to the ICI is essentially proportional to $(\Delta T_0/T)^2$. For given k, the largest contribution comes from the nearest carriers $k' = k+1$ and $k' = k-1$. Taking $k' = k+1$ or $k' = k-1$, the contribution $\bar{P}_{\mathrm{ICI},k}(k')$ increases quadratically with $\mathrm{mod}(k, N_F)$ and becomes maximum for the carriers k that are located closest to the roll-off area, i.e., $k = (N_c-1)/2$ and $k = N_F - (N_c-1)/2$.

The contribution from carrier k' of user ℓ to $\bar{P}_{\mathrm{MUI},k}$ equals $\bar{P}_{\mathrm{MUI},k}(k',\ell) = E_s E[|R_\ell(k,k')|^2]|C_{k,k',\ell}|^2$. For $N_s(N_F+N_p)(\Delta T/T)_{\max} \ll 1$, one obtains

$$\bar{P}_{\mathrm{MUI},k}(k',\ell) \approx \begin{cases} \gamma(k,\ell), & k'=k \\ \zeta(k,k',\ell), & k' \neq k \end{cases} \tag{32}$$

where

$$\begin{aligned} \gamma(k,\ell) &= \frac{E_s B}{N_s-1} (\bmod(k;N_F))^2 \left(\frac{\Delta T_0}{T} - \frac{\Delta T_\ell}{T} \right)^2 \\ \zeta(k,k',\ell) &= \frac{E_s A(k,k') B}{N_s-1} \left(\frac{\Delta T_\ell}{T} \right)^2 \\ &\quad \cdot \left(\bmod(k;N_F) \frac{\Delta T_0}{T} - \bmod(k';N_F) \frac{\Delta T_\ell}{T} \right)^2 \\ B &= \frac{1}{3} \left(\pi N_s \frac{N_F+N_p}{N_F} \right)^2. \end{aligned} \tag{33}$$

As $|C_{k,k,\ell}|^2 \gg |C_{k,k',\ell}|^2$ for $k' \neq k$, the MUI is dominated by the contributions $\bar{P}_{\mathrm{MUI},k}(k',\ell)$, which are largest for the carriers k closest to the roll-off area.

As B is proportional to the square of N_s, the sum $\bar{P}_{\mathrm{ICI},k} + \bar{P}_{\mathrm{MUI},k}$ is dominated by the MUI caused by the symbols transmitted by the nonreference users on carrier k. Assuming that the clock frequency offsets $\Delta T_\ell/T$ of the interfering users are uniformly distributed in the interval $[-(\Delta T/T)_{\max}, (\Delta T/T)_{\max}]$, one obtains

$$\begin{aligned} \bar{P}_{\mathrm{ICI},k} + \bar{P}_{\mathrm{MUI},k} &\approx \bar{P}_{\mathrm{MUI},k} \\ &\approx E_s B \frac{N_u-1}{N_s-1} (\bmod(k;N_F))^2 \\ &\quad \cdot \left(\left(\frac{\Delta T_0}{T} \right)^2 + \frac{1}{3} \left(\frac{\Delta T}{T} \right)^2_{\max} \right). \end{aligned} \tag{34}$$

The largest interference occurs when $|\Delta T_0/T| = (\Delta T/T)_{\max}$.

In the case where $N_F(\Delta T/T)_{\max} \ll 1$ (so that a truncated Taylor series of $|C_{k,k',\ell}|^2$ is accurate), but $N_s(N_F+N_p)(\Delta T/T)_{\max} \ll 1$ is no longer valid, a truncated Taylor series of $E[|R_\ell(k,k')|^2]$ is not accurate, and we have to use (28) instead. In this case, taking into account that $U_{k,k',0} < 1$, $\bar{P}_{\mathrm{ICI},k}(k')$ is upper bounded by the right-hand side of (30). Using $U_{k,k',\ell} \ll 1$, the contribution from carrier k' of user ℓ to $\bar{P}_{\mathrm{MUI},k}$ can now be approximated by

$$\bar{P}_{\mathrm{MUI},k}(k',\ell) \approx \begin{cases} \frac{E_s}{N_s-1}, & k'=k \\ \frac{E_s A(k,k')}{N_s-1} \left(\frac{\Delta T_\ell}{T} \right)^2, & k' \neq k \end{cases}. \tag{35}$$

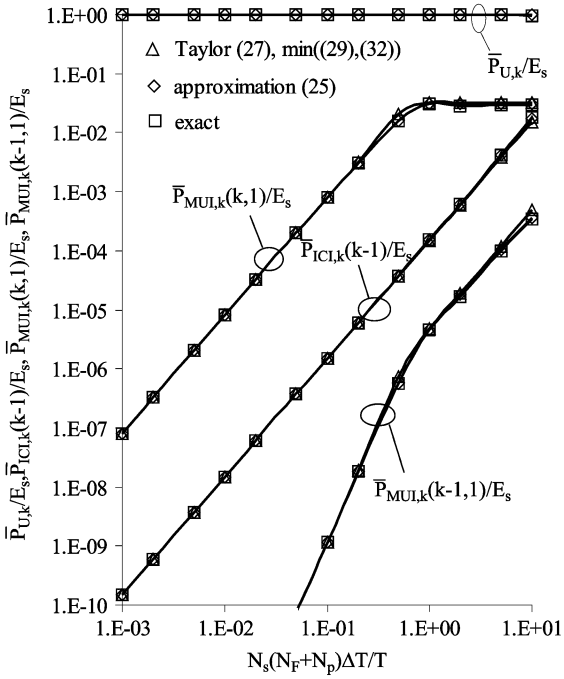

Fig. 8. ICI contribution $P_{\mathrm{ICI},k}(k-1)$ and MUI contributions $P_{\mathrm{MUI},k}(k,1)$ and $P_{\mathrm{MUI},k}(k-1,1), N_F = 64, N_p = 5, N_c = 57, N_s = 32, \Delta T_0/T = -\Delta T_1/T = \Delta T/T, k = (N_c-1)/2$.

Again, $\bar{P}_{\mathrm{ICI},k} + \bar{P}_{\mathrm{MUI},k}$ is dominated by the sum of the contributions $\bar{P}_{\mathrm{MUI},k}(k,\ell)$ from the $N_u - 1$ nonreference users, and its average over the distribution of $\Delta T_\ell/T$ is given by

$$\bar{P}_{\mathrm{ICI},k} + \bar{P}_{\mathrm{MUI},k} \approx \bar{P}_{\mathrm{MUI},k} \approx E_s \frac{N_u-1}{N_s-1}. \tag{36}$$

In order to illustrate the validity of the various approximations, we show in Fig. 8 the quantities $\bar{P}_{U,k}, \bar{P}_{\mathrm{MUI},k}(k,1)$, $\bar{P}_{\mathrm{MUI},k}(k-1,1)$, and $\bar{P}_{\mathrm{ICI},k}(k-1)$, for $k = (N_c-1)/2$ and $\Delta T_0/T = -\Delta T_1/T = \Delta T/T$. The following curves are presented:

- Exact values, based on the computation of the averages in (26), that take into account the possible jumps of the timing offset at the edges of the FFT blocks; note that these jumps affect $\bar{P}_{\mathrm{MUI},k}(k,1)$, $\bar{P}_{\mathrm{MUI},k}(k-1,1)$, and $\bar{P}_{\mathrm{ICI},k}(k-1)$, but not $\bar{P}_{U,k}$. These exact values correspond to $[x_{\min}, x_{\max}] = [-1,+1]$;
- Approximations based on the correct expression (21) of $C_{k,k',\ell}$ and on the approximation (27) that ignores the possible jumps of the timing offset;
- Truncated Taylor series, i.e., (30) for ICI, the minimum value resulting from (32) and (35) for MUI, and $P_{U,k} \approx E_s$ for the useful component.

We observe that both the approximation [based on (21) and (27)] and the truncated Taylor series yield results that nearly coincide with the exact values that take possible jumps of the timing offset into account. This indicates that the effect of these jumps can be safely ignored so that the quantities $x_{\min}$ and $x_{\max}$ do not affect the performance. Moreover, the contributions $\bar{P}_{U,k}, \bar{P}_{\mathrm{MUI},k}(k,1), \bar{P}_{\mathrm{MUI},k}(k-1,1)$, and $\bar{P}_{\mathrm{ICI},k}(k-1)$ are accurately approximated by the simple expressions resulting from the Taylor series expansion.

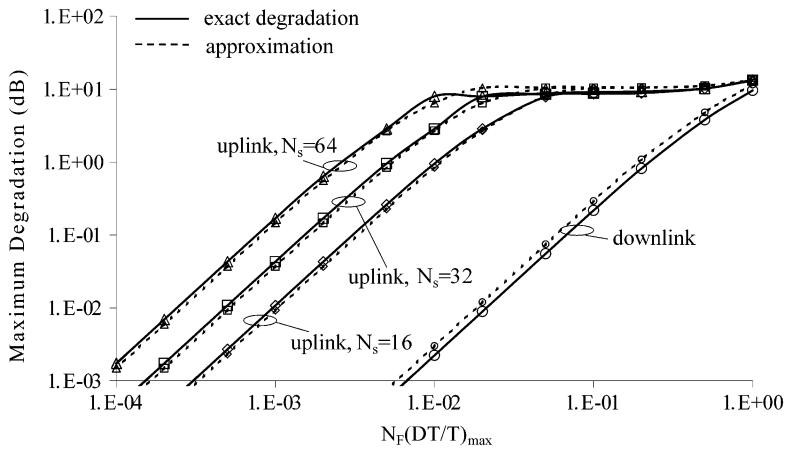

Fig. 9. Maximum degradation in presence of clock frequency offset ($N_F = 64, N_p = 5, N_c = 57, \Delta T_0/T = \Delta T/T = (\Delta T/T)_{\max}, (N_F/N_F + N_p)(E_s/N_0) = 10$ dB).

Fig. 9 shows the maximum (over k) of the degradation of the SINR, assuming a full load ($N_u = N_s$), $\Delta T_0/T = (\Delta T/T)_{\max}$ and a uniform distribution in the interval $[-(\Delta T/T)_{\max}; (\Delta T/T)_{\max}]$ of the clock frequency offsets $\Delta T_\ell/T$ of the nonreference users. We present not only the exact result (which considers all ICI and MUI contributions and takes into account the possible jumps of the timing offset at the edges of the FFT blocks) but the simple approximation as well, which is obtained by taking the minimum of the expressions (34) and (36) for $k = (N_c - 1)/2$. The accuracy of the approximate result indicates that the degradation in the uplink is largest on the carrier $k = (N_c - 1)/2$ (the same degradation occurs on carrier $k = N_F - (N_c - 1)/2$) and is mainly caused by the nonreference users' symbols transmitted on the same carrier. For $N_s(N_F + N_p)(\Delta T/T)_{\max} < 1$, the degradation is according to the approximation (34) and increases quadratically with N_s, N_c and $(\Delta T/T)_{\max}$. For $N_s(N_F + N_p)(\Delta T/T)_{\max} > 1$, the approximation (36) is valid, and the degradation is essentially independent of N_s, N_c, and $(\Delta T/T)_{\max}$ (assuming $N_F(\Delta T/T)_{\max} < 1$ so that $\bar{P}_{U,k} \approx E_s$). In order to keep the degradation small (say, less than about 0.1 dB), it is required that $N_s(N_F + N_p)(\Delta T/T)_{\max} \ll 1$.

B. Downlink MC-DS-CDMA

When the receiver of the reference user has a free-running clock with a relative clock frequency offset $\Delta T/T$ as compared to the frequency $1/T$ of the basestation clock, the timing deviation increases linearly with time: $\epsilon_{n,m} = \epsilon_0 + (m + n(N_F + N_p))\Delta T/T$. However, in contrast with the uplink, where the increasing misalignment in time is compensated at the transmitters of the different users, the coarse synchronization in the downlink is performed at the receiver of each user. This implies that the number of samples in the prefix at the receiver is reduced (when $\Delta T/T > 0$) or increased (when $\Delta T/T < 0$), such that the N_F successive samples kept for further processing remain in the region where interference from other blocks is absent. After coarse synchronization, the timing deviation is given by $\epsilon_{n,m} = \epsilon_n + m\Delta T/T$, where $\epsilon_n = M(\epsilon_0 + n(N_F + N_p)\Delta T/T)$ denotes the timing deviation of the first of the N_F samples of the considered block that are processed by the receiver.

The quantities $I_{k,k',\ell}$ for the carriers outside the roll-off area are given by (20) with $\epsilon_{n,\ell}, \Delta T_\ell/T$ and $H_\ell(f)$ substituted by $\epsilon_n, \Delta T/T$ and $H(f)$, respectively, for $\ell = 0, \ldots, N_u - 1$. It follows that $C_{k,k',\ell}$ from (21) is independent of the user index ℓ. In the following, we use the notation $C_{k,k'}$. The quantity $R_\ell(k, k')$ from (23) is the correlation between the sequences $\{\tilde{c}_{n,k',\ell}\}$ and $\{\tilde{c}_{n,k,0}\}$. However, in contrast with the uplink, ϵ_n is independent of the user index ℓ. Hence, it follows from (23) with $k' = k$ that $R_\ell(k, k) = \delta_\ell$: In downlink transmission, symbols transmitted on carrier k to nonreference users do not give rise to interference on the kth FFT output at the receiver of the reference user. This also can be observed in (24): For $k' = k$, the chips $c_{n,\ell}$ and $c_{n,0}$ are rotated over the same angle such that the orthogonality between the different user signals on the same carrier is not affected. For $k' \neq k$, we have $C_{k,k'} \neq 0$ and $R_\ell(k, k') \neq 0$, i.e., user signals on other carriers do give rise to interference on the kth carrier: The orthogonality between the user signals on different carriers is affected by the clock frequency offset. Hence, a clock frequency offset causes both intercarrier and multiuser interference.

We assume that the symbol energy $E_{s,k,\ell}$, which is transmitted by the base station on carrier k to user ℓ, does not depend on k and ℓ. Because of the fading of the WSSUS, this yields $E_{s,k,\ell}E[|H_k|^2] = E_s$, where E_s denotes the symbol energy (irrespective of k and ℓ) at the input of the receiver of the reference user. As for the uplink transmission, we define SINR_k [see (25)], $P_{U,k}, P_{\text{ICI},k}$, and $P_{\text{MUI},k}$ [see (26)] and the associated $\overline{\text{SINR}}_k, \bar{P}_{U,k}, \bar{P}_{\text{ICI},k}$, and $\bar{P}_{\text{MUI},k}$, with $\epsilon_{n,\ell}, \Delta T_\ell/T$ and $H_\ell(f)$ substituted by $\epsilon_n, \Delta T/T$, and $H(f)$, respectively. Similarly as for the uplink, for small values of the clock frequency offset (i.e., without discontinuities of the timing offset at the edges of the FFT blocks), the average $E[|R_\ell(k, k')|^2]$ can be approximated by (27), where $\Delta T_0/T$ and $\Delta T_\ell/T$ are replaced by $\Delta T/T$. Note that $U_{k,k',\ell}$ (28) in the downlink is independent of the user index ℓ and, therefore, will be denoted as $U_{k,k'}$. Taking into account that $U_{k,k} = 1$ for $k \in I_c$ and assuming the maximum load ($N_u = N_s$), we obtain

$$\bar{P}_{\text{ICI},k} + \bar{P}_{\text{MUI},k} = E_s \sum_{k' \in I_c, k' \neq k} |C_{k,k'}|^2. \qquad (37)$$

When $N_s(N_F+N_p)(\Delta T/T)_{\max} \ll 1$, it follows from (27) that $E[|R_0(k,k')|^2] \approx 1$. The resulting ICI contribution is essentially the same as the right-hand side of (37) so that $\bar{P}_{\mathrm{MUI},k} \ll \bar{P}_{\mathrm{ICI},k}$: The degradation is dominated by the ICI, and MUI is virtually absent. For $N_s(N_F+N_p)(\Delta T/T)_{\max} \gg 1$, we see from (27) that $E[|R_\ell(k,k')|^2] \approx 1/(N_s-1)$ for $\ell \neq 0$. Assuming a full load ($N_u = N_s$), the corresponding MUI contribution is essentially the same as the right-hand side of (37): In this case, the total interference is dominated by MUI, and ICI is virtually absent ($\bar{P}_{\mathrm{ICI},k} \ll \bar{P}_{\mathrm{MUI},k}$).

When $N_F(\Delta T/T)_{\max} \ll 1$, (37) can be approximated as

$$\bar{P}_{\mathrm{ICI},k} + \bar{P}_{\mathrm{MUI},k} \approx E_s C(k) \left(\frac{\Delta T}{T}\right)^2 \tag{38}$$

where

$$C(k) = \sum_{k' \in I_c, k' \neq k} A(k,k') \tag{39}$$

and $A(k,k')$ is given by (31). Hence, the interference power is essentially proportional to $(\Delta T/T)^2$. For given $\Delta T/T$, the interference power is independent of the spreading factor. Assuming the clock frequency offset is in the interval $[-(\Delta T/T)_{\max}, (\Delta T/T)_{\max}]$, the interference power becomes maximum when $|\Delta T/T| = (\Delta T/T)_{\max}$. For given k, the interference power (38) depends on the number of modulated carriers as the summation over k' in (38) ranges over the set I_c of N_c modulated carriers. An upper bound on the interference power is obtained by extending in (39) the summation interval over all N_F carriers, i.e., $k' = 0, \ldots, N_F - 1$. This corresponds to replacing in (38) $C(k)$ by $C_{\mathrm{up}}(k)$, which is given by

$$C_{\mathrm{up}}(k) = \sum_{k'=0, k' \neq k}^{N_F-1} A(k,k') \tag{40}$$

which, for given k, is independent of the number N_c of modulated carriers. The quantity $C_{\mathrm{up}}(k)$ can be further simplified by using the approximation

$$C_{\mathrm{up}}(k) \approx C_{\mathrm{appr}}(k) = \frac{\pi^2}{3}(\mathrm{mod}(k; N_F))^2. \tag{41}$$

Fig. 10 shows the coefficients $C(k), C_{\mathrm{up}}(k)$, and $C_{\mathrm{appr}}(k)$ as a function of the carrier index. We observe from the behavior of $C(k)$ that the largest interference in the downlink occurs for carriers near (but not exactly at) the the edge of the roll-off area. The coefficients $C_{\mathrm{up}}(k)$ and $C_{\mathrm{appr}}(k)$ are essentially the same and become maximum for the carriers $k = (N_c-1)/2$ and $k = N_F-(N_c-1)/2$. For carriers that are not close to the edge of the roll-off area, $C_{\mathrm{up}}(k)$ and $C_{\mathrm{appr}}(k)$ are accurate approximations of $C(k)$, and they overestimate $C(k)$ for the other carriers.

Fig. 9 shows the maximum (over k) of the degradation of the SINR obtained with (37), along with the degradation obtained by replacing in (38) $C(k)$ by $C_{\mathrm{appr}}(k)$ for $k = (N_c - 1)/2$. As we observe, the approximation is close to the actual degradation. Hence, the simple expression (41) can be used to compute the degradation caused by a clock frequency offset in the downlink. To obtain small degradations, it is required that $|N_F(\Delta T/T)_{\max}| \ll 1$, in which case, the degradation is proportional to $(N_F(\Delta T/T)_{\max})^2$ and independent of the spreading factor N_s.

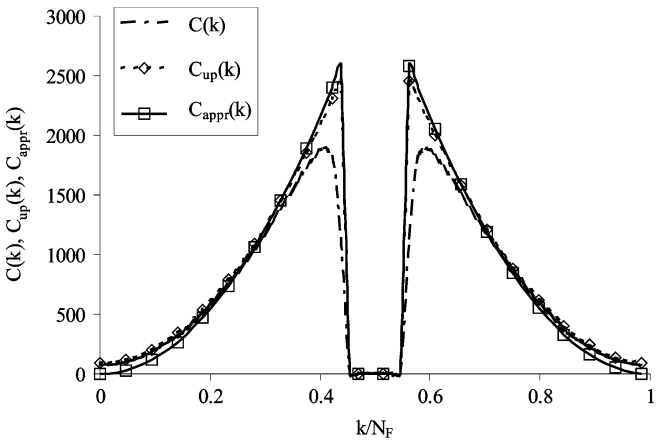

Fig. 10. Coefficients $C(k), C_{\mathrm{up}}(k)$, and $C_{\mathrm{appr}}(k), N_F = 64, N_c = 57$.

We observe that for $|N_F(\Delta T/T)_{\max}| \ll 1$, the maximum degradation is much larger in the uplink than in the downlink. Whereas the ICI contributions $\bar{P}_{\mathrm{ICI},k}(k')$ in the uplink and the downlink are the same, the sum of the MUI contributions $\bar{P}_{\mathrm{MUI},k}(k',\ell)$ is much larger in the uplink than in the downlink. This can be explained by noting that the dominant MUI contributions to carrier k are caused by signals transmitted on carriers k' in the vicinity of k.

- In the downlink, the clock frequency offset is the same for the contributions from all user signals. Hence, the chips (24) on neighboring carriers k and k' are rotated over nearly the same angle so that the orthogonality between the reference user and the other users is only slightly affected. For $k = k'$, the orthogonality is maintained so that $\bar{P}_{\mathrm{MUI},k}(k,\ell)$ is zero.
- In the uplink, the different user signals are affected by different clock frequency offsets. As a result, the chips (24) are rotated over angles that are, on average, larger than in the case of downlink transmission. Consequently, the orthogonality between the reference user and the other users is strongly affected, resulting in a MUI interference power that is substantially larger than in the downlink. In particular, the MUI contributions $\bar{P}_{\mathrm{MUI},k}(k,\ell)$ are the dominant ones.

In the uplink, a small degradation can be obtained only when $N_s N_F(\Delta T/T)_{\max} \ll 1$. As compared to the downlink, this condition on $(\Delta T/T)_{\max}$ is more stringent by a factor of N_s. For $N_s N_F(\Delta T/T)_{\max} \ll 1$, the uplink degradation is essentially proportional to $(N_s N_F(\Delta T/T)_{\max})^2$; in this region, the ratio between uplink and downlink degradation is proportional to $(N_s)^2$.

V. Conclusion

In this paper, we have investigated the effect of fixed timing offsets and clock frequency offsets on uplink and downlink MC-DS-CDMA with orthogonal spreading sequences on multipath fading channels. We have derived simple analytical expressions that closely approximate the performance degradation. Our conclusions can be summarized as follows.

- Constant timing offsets give rise to performance degradation for neither uplink MC-DS-CDMA nor downlink MC-DS-CDMA.
- Clock frequency offsets give rise to a reduction of the useful component and to the occurrence of both ICI and MUI.
- For both the uplink and the downlink, the degradation caused by a clock frequency offset strongly increases with $N_F(\Delta T/T)_{\max}$.
- For given $N_F(\Delta T/T)_{\max}$, the degradation in the downlink does not depend on the spreading factor and is essentially proportional to $(N_F(\Delta T/T)_{\max})^2$; this degradation is caused mainly by ICI. Assuming full load, the degradation in the uplink is caused mainly by MUI and increases with an increasing spreading factor. The degradation in the uplink is larger than in the downlink because the uplink is affected by a larger amount of MUI and is essentially proportional to $(N_s N_F(\Delta T/T)_{\max})^2$

It can be verified from [10] and [11] that the degradation for downlink MC-DS-CDMA is the same as the corresponding degradation for OFDM and essentially the same as the degradation for downlink MC-CDMA, assuming the three multicarrier systems have the same carrier spacing.

References

[1] R. van Nee and R. Prasad, *OFDM for Wireless Multimedia Communications*. Norwell, MA: Artech House, 2000.

[2] Z. Wang and G. B. Giannakis, "Wireless multicarrier communications," *IEEE Signal Process. Mag.*, vol. 17, no. 3, pp. 29–48, May 2000.

[3] N. Morinaga, M. Nakagawa, and R. Kohno, "New concepts and technologies for achieving highly reliable and high capacity multimedia wireless communication systems," *IEEE Commun. Mag.*, vol. 38, no. 1, pp. 34–40, Jan. 1997.

[4] L. Hanzo, M. Münster, B. J. Choi, and T. Keller, *OFDM and MC-CDMA for Broadband Multi-User Communications, WLAN's and Broadcasting*. New York: Wiley, 2003.

[5] S. Hara and R. Prasad, *Multicarrier Techniques for 4G Mobile Communications*. Norwell, MA: Artech House, 2003.

[6] ——, "Overview of multicarrier CDMA," *IEEE Commun. Mag.*, vol. 35, no. 12, pp. 126–133, Dec. 1997.

[7] J.-P. Linnartz, "Performance analysis of synchronous MC-CDMA in mobile Rayleigh channel with both delay and Doppler spreads," *IEEE Trans. Veh. Technol.*, vol. 50, no. 6, pp. 1375–1387, Nov. 2001.

[8] Z. Hou and V. K. Dubey, "Exact analysis for downlink MC-CDMA in Rayleigh fading channels," *IEEE Commun. Lett.*, vol. 8, no. 2, pp. 90–92, Feb. 2004.

[9] Q. Shi and M. Latva-Aho, "Spreading sequences for asynchronous MC-CDMA revisited: Accurate bit error rate analysis," *IEEE Trans. Commun.*, vol. 51, no. 1, pp. 8–11, Jan. 2003.

[10] C. W. You and D. S. Hong, "Multicarrier CDMA systems using time-domain and frequency-domain spreading codes," *IEEE Trans. Commun.*, vol. 51, no. 1, pp. 17–21, Jan. 2003.

[11] X. Gui and T. S. Ng, "Performance of asynchronous orthogonal multicarrier CDMA system in frequency selective fading channel," *IEEE Trans. Commun.*, vol. 47, no. 7, pp. 1084–1091, Jul. 1999.

[12] L.-L. Yang and L. Hanzo, "Multicarrier DS-CDMA: A multiple access scheme for ubiquitous broadband wireless communications," *IEEE Commun. Mag.*, vol. 41, no. 10, pp. 116–124, Oct. 2003.

[13] S. Kondo and L. B. Milstein, "Performance of Multicarrier DS-CDMA systems," *IEEE Trans. Commun.*, vol. 44, no. 2, pp. 238–246, Feb. 1996.

[14] L. Hanzo, L.-L. Yang, E.-L. Kuan, and K. Yen, *Single and Multi-Carrier DS-CDMA: Multi-User Detection, Space-Time Spreading, Synchronization, Networking and Standards*. New York: Wiley, 2003.

[15] Q. Chen, E. S. Sousa, and S. Pasupathy, "Multicarrier CDMA with adaptive frequency hopping for mobile radio systems," *IEEE J. Sel. Areas Commun.*, vol. 14, no. 9, pp. 1852–1858, Dec. 1996.

[16] L.-L. Yang and L. Hanzo, "Performance of generalized multicarrier DS-CDMA over Nakagami-m fading channels," *IEEE Trans. Commun.*, vol. 50, no. 6, pp. 956–966, Jun. 2002.

[17] V. M. DaSilva and E. S. Sousa, "Multi-carrier orthogonal CDMA codes for quasisynchronous communication systems," *IEEE J. Sel. Areas Commun.*, vol. 12, no. 5, pp. 842–852, Jun. 1994.

[18] E. A. Sourour and M. Nakagawa, "Performance of orthogonal multicarrier CDMA in a multipath fading channel," *IEEE Trans. Commun.*, vol. 44, no. 3, pp. 356–367, Mar. 1996.

[19] A. M. Gallardo, M. E. Woodward, and J. Rodriguez-Tellez, "Performance of DVB-T OFDM based single frequency networks: Effects of frame synchronization, carrier frequency offset, and nonsynchronised sampling errors," *Proc. VTC Fall*, pp. 962–966, Oct. 2001.

[20] G. Malmgren, "Impact of carrier frequency offset, doppler spread, and time synchronization errors in OFDM based single frequency networks," in *Proc. Globecom*, Nov. 1996, pp. 729–733.

[21] H. Steendam and M. Moeneclaey, "The effect of carrier frequency offsets on downlink and uplink MC-DS-CDMA," *IEEE J. Sel. Areas Commun.*, vol. 19, no. 12, pp. 2528–2536, Dec. 2001.

[22] K. Ko, T. Kim, and D. Hong, "Performance evaluation of asynchronous MC-CDMA systems with an effect of carrier-frequency offsets," in *Proceedings ICC*, May 2003, pp. 3447–3451.

[23] L. Tomba and W. A. Krzymien, "Sensitivity of the MC-CDMA access scheme to carrier phase noise and frequency offset," *IEEE Trans. Veh. Technol.*, vol. 48, no. 5, pp. 1657–1665, Sep. 1999.

[24] K. Sathanantan and G. Tellambura, "Probability of error calculation of OFDM systems with frequency offset," *IEEE Trans. Commun.*, vol. 49, no. 11, pp. 1884–1888, Nov. 2001.

[25] T. Pollet, P. Spruyt, and M. Moeneclaey, "The BER performance of OFDM systems using nonsynchronized sampling," in *Proc. Globecom*, San Francisco, CA, Nov. 1994, pp. 253–257.

[26] H. Steendam and M. Moeneclaey, "Sensitivity of orthogonal frequency-division multiplexed systems to carrier and clock synchronization errors," *Signal Process.*, vol. 80, no. 7, pp. 1217–1229, 2000.

[27] ——, "The sensitivity of MC-CDMA to synchronization errors," *Eur. Trans. Telecommun., Special Issue MC-SS*, vol. 10, no. 4, pp. 429–436, Jul.–Aug. 1999.

[28] ——, "The effect of clock frequency offsets on downlink MC-DS-CDMA," in *Proc. IEEE Int. Symp. Spread Spectrum Techn. Applicat.*, Prague, Czech Republic, Sep. 2–5, 2002, pp. 113–117.

[29] J. G. Proakis, *Digital Communications*. New York: McGraw-Hill, 2000.

Heidi Steendam received the diploma in electrical engineering and the Ph.D. degree in electrical engineering from Ghent University, Gent, Belgium, in 1995 and 2000, respectively.

She is a Professor with the Department of Telecommunications and Information Processing (TELIN), Ghent University. Her main research interests are in statistical communication theory, carrier and symbol synchronization, bandwidth-efficient modulation and coding, spread-spectrum (multicarrier spread-spectrum), and satellite and mobile communication. She is the author of more than 60 scientific papers in international journals and conference proceedings.

Prof. Steendam has been an executive Committee Member of the IEEE Communications and Vehicular Technology Society Joint Chapter, Benelux Section, since 2002. She has been active in various international conferences as Technical Program Committee member and Session chair.

Herwig Bruneel was born in Zottegem, Belgium, in 1954. He received the M.S. degree in electrical engineering, the degree of Licentiate in computer science, and the Ph.D. degree in computer science in 1978, 1979, and 1984, respectively, all from Ghent University, Gent, Belgium.

He is a Full-Time Professor with the Faculty of Applied Sciences and Head of the Department of Telecommunications and Information Processing, Ghent University, where he also leads the SMACS Research Group. His main personal research interests include stochastic modeling and analysis of communication systems, discrete-time queueing theory, and the study of ARQ protocols. He has published more than 200 papers on these subjects and is coauthor of the book, with B. G. Kim, "Discrete-Time Models for Communication Systems Including ATM" (Boston, MA: Kluwer, 1993). From October 2001 to September 2003, he served as the Academic Director for Research Affairs at Ghent University.

Marc Moeneclaey received the diploma in electrical engineering and the Ph.D. degree in electrical engineering from the University of Ghent, Gent, Belgium, in 1978 and 1983, respectively.

From 1978 to 1999, at Ghent University, he held various positions for the Belgian National Fund for Scientific Research (NFWO), from Research Assistant to Research Director. He is presently a Professor with the Department of Telecommunications and Information Processing (TELIN), Ghent University. His research interests include statistical communication theory, carrier and symbol synchronization, bandwidth efficient modulation and coding, spread-spectrum, and satellite and mobile communication. He is the author of more than 200 scientific papers in international journals and conference proceedings. Together with Prof. H. Meyr (RWTH Aachen) and Dr. S. Fechtel (Siemens AG), he co-authored the book *Digital Communication Receivers—Synchronization, Channel Estimation, and Signal Processing* (New York: Wiley, 1998).

Dr. Moeneclaey served as Editor for *Synchronization* and for the IEEE TRANSACTIONS ON COMMUNICATIONS from 1992 to 1994. He was co-guest editor for the December 2001 IEEE Special Issue on Signal Synchronization in Digital Transmission Systems of the IEEE JOURNAL OF SELECTED AREAS IN COMMUNICATIONS. From 1993 to 2002, he has been an executive Committee Member of the IEEE Communications and Vehicular Technology Society Joint Chapter, Benelux Section. He has been active in various international conferences as Technical Program Committee member and Session chairman.